Environ. Eng. Res. 2016; 21(3): 291-296
http://dx.doi.org/10.4491/eer.2016.016
pISSN 1226-1025
eISSN 2005-968X

Photocatalytic removal of NO_x using TiO_2-coated zeolite

Joseph Albert Mendoza, Dong Hoon Lee, Joo-Hyon Kang[†]

Department of Civil and Environmental Engineering, Dongguk University-Seoul Campus, 26 Pil-dong 3-ga, Jung-gu, Seoul 04620, Republic of Korea

ABSTRACT

Application of photocatalytic nanoparticles has been recently gaining an increased attention as air purifying material for sustainable urban development. The present work reports the photocatalytic removal of gaseous phase nitrogen oxides (NO_x) using TiO_2–coated zeolite to be applied as a filter media for the urban green infrastructure such as raingardens. The TiO_2–coated zeolite was synthesized by simple wet chemistry method and tested in a continuous-flow photo-reactor for its removal efficiency of NO_x under different conditions of the weight percentage of TiO_2 coated on the zeolite, and gas retention time. The removal efficiency of NO_x in general increased as the weight percentage of TiO_2 coated on the zeolite increased up to 15-20%. Greater than 90% of NO_x was removed at a retention time of one minute using the TiO_2–coated zeolite (TiO_2 weight percentage = 20%). Overall, TiO_2–coated zeolite showed greater efficiency of NO_x removal compared to TiO_2 powder probably by providing additional reaction sites from the porous structure of zeolite. It was presumed that the degradation of NO_x is attributed to both the physical adsorption and photocatalytic oxidation that could simultaneously occur at the catalyst surface.

Keywords: Nanoparticles, NO_x, Photocatalysis, TiO_2, Zeolite

1. Introduction

Nitrogen monoxide (NO) and dioxide (NO_2), which are collectively called nitrogen oxides(NO_x) are harmful and poisonous gases that are emitted mainly from anthropogenic sources such as industrial power plants and automobile engines [1-2]. Air pollution caused by photochemical oxidants, such as ozone and NO_x, is one of the serious problems faced by urban areas [3]. The annual mean concentrations of NO_x in urban areas globally are in the range of 20-90 ppb but hourly averages can often exceed 1000 ppb on heavy vehicular traffic conditions [4]. NO_x has significant impacts on the environment, human and animal health, and plant vegetation. Adverse effects of NO_x include acid rain, photochemical smog, ozone layer depletion, greenhouse effect, and ecological toxification [5]. Furthermore, NO_x has been also a recurring problem of worsening indoor air quality (IAQ) in most building structures, and diseases related to lower IAQ have been reported [6]. Recent study done by Shakerkhatibi, et al. (2015) [7] showed that gaseous air pollutants of NO_2, NO, and CO were associated with the hospital admissions for chronic obstructive pulmonary disease.

The needs for mitigating the negative effects of NO_x have increased over the past few decades. Photocatalytic oxidation (PCO) has been suggested as an efficient and cost effective approach to control airborne pollutants such as NO_x [8]. PCO relies on photocatalysts which utilize ultraviolet (UV) light radiation from sunlight or artificial light assisting in oxidizing various pollutants [9]. Among the photocatalysts used in PCO processes, titanium dioxide (TiO_2) has been most widely used because of its chemical stability, non-toxicity, and relatively low cost [10-11]. In addition, TiO_2 nanoparticles are able to provide more active sites than standard TiO_2 powder [12], making the degradation of pollutants more effective. Upon irradiation of UV light, TiO_2 generates electrons and holes in the conduction and valence bands, respectively which could participate in the oxidation-reduction (redox) reactions for pollutant degradation [13-15]. The proposed mechanism of NO_x photocatalytic oxidation consist of three stages: NO initially reacts with the OH- radical formed from the TiO_2 surface reaction of H_2O and oxygen, resulting in HNO_2 (first stage) before subsequently becoming HNO_3 (second stage) that would be desorbed at the TiO_2 surface, and thus regenerating the catalyst (third stage). The mechanisms were described in more detail by various researchers [16-18].

Since the first discovery of super-hydrophilicity of TiO_2 by Fujishima, *et al.* (2000) [19], TiO_2 has been applied to building materials with the aim of air cleaning, self-cleaning, and anti-fogging functions [20-23]. Recent applications of TiO_2 has been widen to the outdoor building materials such as pavements and concrete surfaces to control urban airborne pollutants such as NO_x [18, 23-28]. The present study is a preliminary study to eventually propose the application of photocatalytic nanoparticles to the surface media layer (*i.e.* zeolite) of urban green infrastructure practices such as

Received January 28, 2016 **Accepted** April 27, 2016

[†] Corresponding author
Email: joohyon@dongguk.edu
Tel: 82-2-2260-3776 Fax: 82-2-2266-8753

rain gardens, providing multiple functions of controlling air and water quality in urban settling. Rain garden, or also called as bio-retention area, is one of the urban stormwater management practices recommended by the United States' Environmental Protection Agency (US EPA) since 2000 [29]. Rain gardens are low depressions in the landscape that are planted with trees and/or shrubs, and covered with a bark mulch layer or ground cover allowing for the infiltration of storm water to recharge aquifers, and reduce surface runoffs. Various designs have been developed for rain garden systems [30] but researches on the use of nanoparticles on stormwater management practices are limited in number [24-26, 31-32].

The scope of the present research is directed on identifying the effectiveness of applying TiO_2 nanoparticles on natural zeolites, which will be added within the rain garden system, for adding function of NO_x removal from the urban atmosphere. The photocatalytic removal of NO_x in air was investigated thru a lab-scale continuous flow reactor with TiO_2 coated onto natural zeolite as a preliminary study for its applicability to actual rain garden systems.

2. Materials and Methods

2.1. Synthesis of the Nanoparticle-coated Zeolite

Natural zeolite (DAEJUNG Chemicals, Korea) with a mean diameter of 3 mm was calcined at 600°C for 2 h to remove any organic impurities present, and subsequently cooled at room temperature. Then, the prepared zeolite was added to a flask with an aqueous suspension of TiO_2 (DAEJUNG Chemicals, Korea) nanoparticles (mean diameter was 300 nm), and was shaken at 150 rpm for 2 h to ensure homogenous coating of the TiO_2 nanoparticles on the zeolite surface. Finally the mixed solution was oven dried at 105oC for 24 h followed by calcination at 600oC for 2 h, producing the TiO_2-coated zeolite. Scanning electron microscope (SEM; JEOL-7800F, JEOL, Japan) with Energy Dispersive X-ray Spectrometer (EDS) and X-ray diffractometer (XRD; Ultima IV, Rigaku, Japan) were conducted to characterize the morphology, composition, and crystallinity of the TiO_2-coated zeolite. Surface area measurements were carried out using the BET analysis method (Autosorb-iQ 2ST/MP, Quantachrome, U.S.A.).

2.2. Photocatalytic NO_x Degradation Experiments

A continuous-flow photo-reactor was used to measure the performance of the TiO_2-coated zeolite in removing NO_x in the air. Fig. 1 shows the laboratory setup consisting of NO_x source (5 ppm NO in N_2, DONG-AH Gas, Korea), purified air source (< 1% hydrocarbon impurities, DONG-AH Gas, Korea), flow controllers (DWYER, USA), box-type photo-reactor (made of acryl), UV-A lamp (20 W, SANKYO DENKI, Japan) and a chemiluminiscent NO_x analyzer (ECOTECH, SERINUS 40, Australia). Either of the two photo-reactors with different dimensions (Reactor 1: L = 310 mm, W = 110 mm, H = 55, Reactor 2: L = 600 mm; W = 220 mm; H = 100 mm) was used when appropriate for the convenience of adjusting the gas retention time of the reactor to a required value during the test. A total of 6 UV-A lamps (20 W each with light intensity of 0.38 mW/cm^2) were simultaneously used to provide sufficient light energy for the photocatalytic reaction.

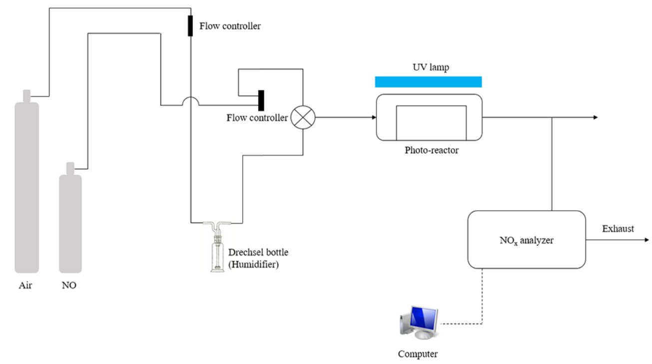

Fig. 1. Schematic of the laboratory setup for the NO_x removal experiment.

An appropriate amount of the TiO_2-coated zeolite was loaded into the reactor and then the reactor was carefully sealed. Afterwards, the NO containing nitrogen gas and the purified air were allowed to flow into the reactor at flow rates of 0.2 L/min and 2 L/min, respectively, until equilibrium NO_x concentration in the inflow has achieved. The purified air was passed through a humidifier before being mixed with NO containing nitrogen gas in order to achieve a required level of relative humidity (40-60%) in the reactor. The gas flow was continued for 30 minutes before the light source was turned on. Afterwards, the TiO_2-coated zeolite was irradiated for 60 minutes during which the NO_x concentration of the outflow gas was recorded at 1 min intervals by the NO_x analyzer. After the one hour of irradiation, the light source was turned off and then the gas valves were closed. All experiments were conducted at ambient temperature (18-20°C). The detailed experimental procedure can be referred to published literatures [25-27, 31-32] and the ISO 22197-1:2007 standard for air purification performance of semiconducting photocalytic materials [33].

3. Results and Discussion

3.1. Characterization of the Synthesized Coated Zeolite

The scanning electron microscope (SEM) and energy dispersive X-ray spectrometer (EDS) images of the TiO_2-coated zeolite were presented in Fig. 2. The TiO_2 nanoparticles are fairly distributed on the zeolite surface but particle agglomerations were often observed on the zeolite surface probably due to the sintering of TiO_2 particles at high temperature calcination [33, 36]. However, it should be mentioned that the controlled distribution of guest particles (TiO_2) with minimal particle agglomeration on the host particle surface (zeolite) is still an active research in the nanotechnology field [8, 12-13, 18-19]. The EDS scan confirmed that TiO_2 particles were present on the zeolite surface based on the detected elements. The major peak of Ti at ~4.5 keV seen on the EDS spectrum represents the binding energy for the Ti4+ oxidation present in most TiO_2 phases (such as anatase, rutile, and brookite). The crystal structure of the synthesized coated zeolite was examined using XRD. The diffraction peaks matched with that of tetragonal anatase TiO_2 (a = 3.7892 Å, c = 9.5370 Å; Crystallography Open Database, No. 5000223) indicating that TiO_2 was successfully loaded on the zeolite surface as shown in Fig. 3.

The BET surface listed in Table 1 exhibits a decrease in surface area when TiO_2 was coated in zeolite. This could be due to the decrease of zeolite mesopore sites where N2 gas was adsorbed, which is also an indication of a successful coating of the zeolite surface with the TiO_2 nanoparticles. However, the decreased in BET surface area (i.e., mesopores) had negligible effects to the pollutant removal efficiency of the coated zeolite.

Table 1. BET Surface Area of the Tio₂ Coated Zeolite and Bare Zeolite

Catalyst	BET Surface Area, m^2/g
TiO_2 coated zeolite	80.593
Zeolite only	208.782

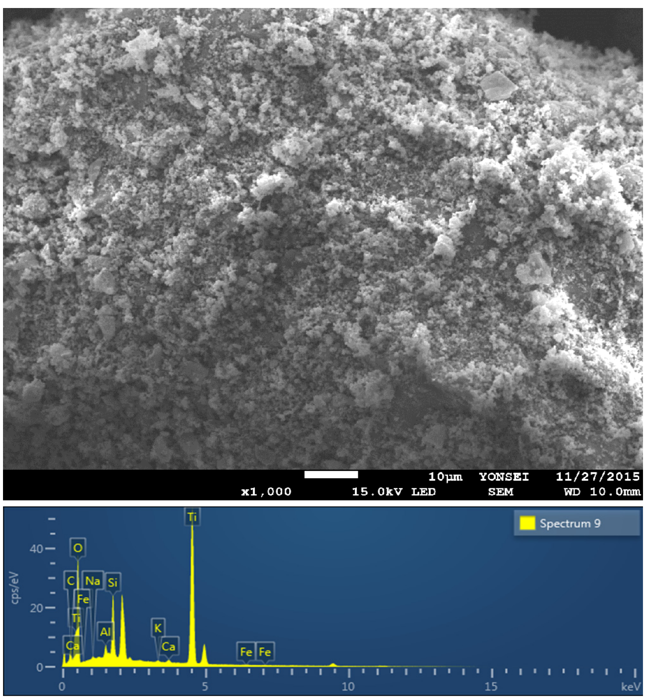

Fig. 2. Scanning electron microscope (SEM) and the energy dispersive X-ray spectrometer images for the TiO_2 coated zeolite.

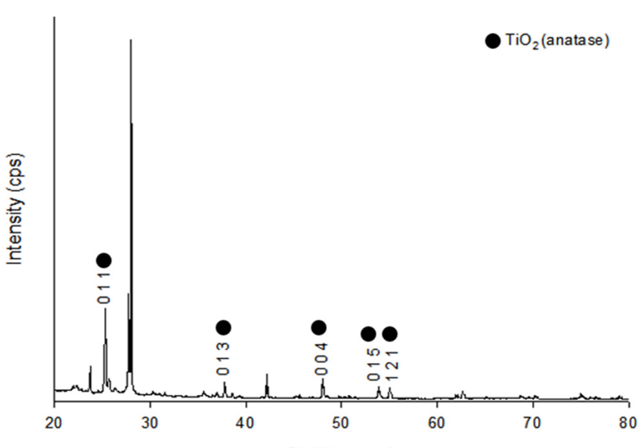

Fig. 3. X-ray diffraction pattern for the TiO_2-coated zeolite.

3.2. Effect of TiO_2 Particles in the Photocatalytic NO_x Degradation

Preliminary experiments were performed using TiO_2 particles only as shown in Fig. 4. After the UV lamp was turned on, an immediate decrease in the NO and NO_x concentration was observed. NO concentration remained constant throughout the irradiation period of one hour while NO_x (NO + NO_2) concentration gradually increased due to the increased concentration of NO_2 created from the oxidation of NO. The NO_x removal efficiency (R.E.) was calculated using Eq. (1).

$$\%R.E. = \frac{(C_o - C_{Ave})}{C_o} \times 100\% \tag{1}$$

where C_{ave} is the average concentration of NO_x in the outflow during the one hour of irradiation, and C_0 is the NO_x concentration of the inflow. Before the light source was turned on, no significant change in the pollutant gas was observed, indicating that the chemical transformation of NO_x can be attributed to the photocatalytic mechanism [10, 13-14]. The calculated NO_x and NO removal efficiencies based on the concentration profile from Fig. 4 were 48% and 64%, respectively, which are similar to most of the previously reported values in the literature [18, 20, 26-28, 31-32]. When the light source was turned off after the one hour of irradiation, NO_x concentration immediately returned to its initial value, indicating no permanent physical adsorption of NO_x on the photocatalyst particles.

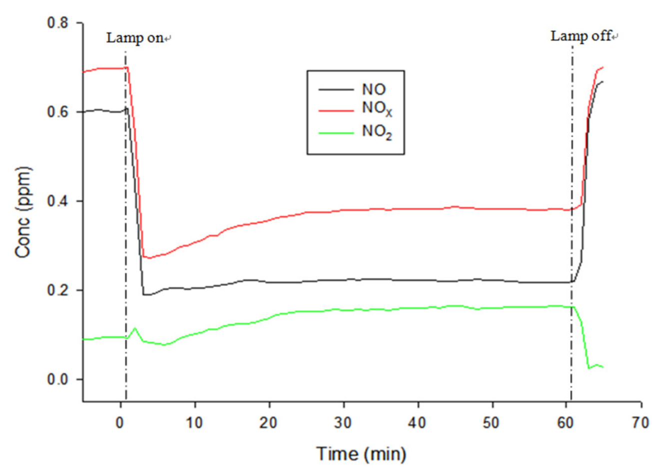

Fig. 4. Example of the NO_x concentration profile with respect to time during photocatalytic experiments.

3.3. Role of Zeolite in the Photocatalytic Degradation

The removal efficiency generally improved when TiO_2 was coated onto natural zeolite as shown in Fig. 5. The improved efficiency can be due to the capability of zeolite to act as adsorbent for the nitrate (NO_3^-) evolved from the photocatalytic oxidation of NO_x. Zeolite can also provide for increased active sites for NO gas to react with TiO_2 because of its porous structure [35, 36]. That is zeolite can assist TiO_2 nanoparticles in capturing the target pollutants for the subsequent photocatalytic reactions [37-39].

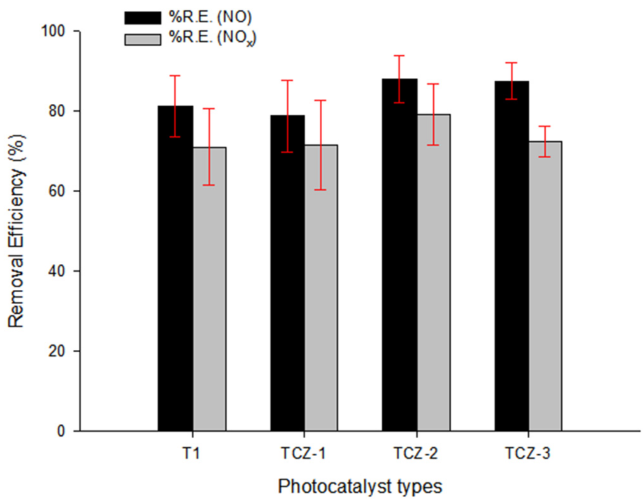

Fig. 5. Comparison of the NO_x degradation performance between TiO_2 nanoparticles and TiO_2 coated zeolite. Notes: T1 = TiO_2 powders under UV-A irradiation; TCZ-1 = TiO_2 (10 wt.%) coated zeolite; TCZ-2 = TiO_2 (15 wt.%) coated zeolite; TCZ-3 = TiO_2 (20 wt.%) coated zeolite. Error bars indicate standard deviations of four replicate experiments.

A control test was performed; the uncoated natural zeolite was placed inside the photo-reactor and subjected to the same irradiation procedure, and no significant change was observed in the NO_x concentration, indicating that there is a synergistic effect with the addition of TiO_2 for the efficient removal of NO_x.

3.4. Effect of Varying TiO_2 Mass Loadings in Zeolite Media

Three TiO_2-coated zeolite with different TiO_2 weight percentages (*i.e.* 10 wt.%, 15 wt.%, and 20 wt.%) were compared in terms of the NO_x removal efficiency. Overall, as the weight percentage of TiO_2 with respect to zeolite increased, the removal efficiency also increased, which might be due to the increased active sites for photocatalytic reactions in the media. However, variances were observed in the removal efficiency among different replicate samples of the coated zeolite, which could be due the uneven distribution of the TiO_2 particles over the zeolite aggregates during the coating process. The variation in NO_x removal efficiency among different replicate samples decreased as the mass percentages of TiO_2 increased due probably to the increased probability of the TiO_2 particles to be well distributed over the zeolite aggregates. Therefore, the TiO_2-coated zeolite with 20 wt.% TiO_2 was used for the subsequent photocatalytic experiments.

3.5. Effect of Gas Retention Time in the Photocatalytic Degradation

Fig. 6 shows the removal efficiencies of NO_x using the coated TiO_2-zeolite at different gas retention times. The removal efficiency increased as the gas retention time increased. Lower retention time values have lesser time for the pollutant gas to come into contact with the TiO_2 catalyst and thereby reducing its efficiency. Greater than 90% of NO_x was removed at a retention time of one minute using the TiO_2-coated zeolite (TiO_2 weight percentage = 20%).

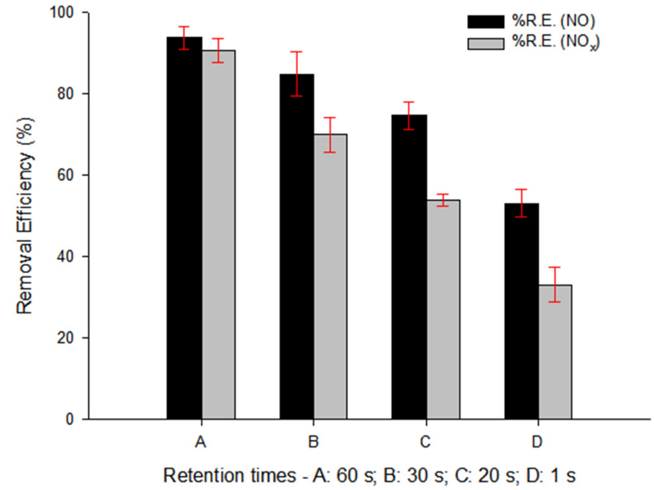

Fig. 6. Effect of retention time on the removal efficiency for (20 wt.%) TiO_2 coated zeolite. Error bars indicate standard deviations of four replicate experiments

4. Conclusions

The effectiveness of coating TiO_2 particles into natural zeolite has been demonstrated in this study. Generally, the removal efficiency of NO_x increased as the weight percentage of TiO_2 coated on the zeolite but variances in the NO_x removal were observed among different replicate samples of the coated zeolite, which could be due to the uneven TiO_2 distribution on the zeolite aggregates during the coating process. Overall, TiO_2-coated zeolite showed greater efficiency compared to TiO_2 powder probably because zeolite can provide additional reaction sites from its porous structure. The degradation of NO_x have been attributed to both the physical adsorption and photocatalytic mechanisms simultaneously happening on the catalyst surface. A proportional relationship was also seen between the removal efficiency and retention time as well. Sufficient contact time with the particles would be required to ensure adsorption and degradation of the pollutant. More than 90% of NO_x was removed at a retention time of one minute using the TiO_2-coated zeolite (with TiO_2 weight percentage at 20%).

Acknowledgments

This research was supported by a grant (14CTAP-C086804-01) from the Technology Advancement Research Program funded by the Ministry of Land, Infrastructure and Transport of the Korean government.

References

1. Lin JT, McElroy MB, Boersma KF. Constraint of anthropogenic NO_x emissions in China from different sectors: A new methodology using multiple satellite retrievals. *Atmos. Chem. Phys.* 2010;10:63-78.

2. Roy S, Hegde MS, Madras G. Catalysis for NO_x abatement. *Appl. Energ.* 2009;86:2283-2297.
3. Venkanna R, Nikhil GN, Siva Rao T, Sinha PR, Swamy YV. Environmental monitoring of surface ozone and other trace gases over different time scales: chemistry, transport and modeling. *Int. J. Environ. Sci. Technol.* 2015;12:1749-1758.
4. The World Bank Group, United Nations Environment Programme, and United Nations Industrial Development Organization. Pollution Prevention and Abatement Handbook 1998: Toward Cleaner Production. Washington D.C.:World Bank; 1999. p. 223-226.
5. Lebowitz MD, Walkinshaw DS. Indoor Air '90: Health effects associated with indoor air contaminants. *Arch. Environ. Health.* 1992;47:6-7.
6. Baek S, Kim Y, Perry R. Indoor air quality in homes, offices and restaurants in Korean urban areas indoor outdoor relationships. *Atmos. Environ.* 1997;31:529-544.
7. Shakerkhatibi M, Dianat I, Asghari Jafarabadi M, Azak R, Kousha A. Air pollution and hospital admissions for cardiorespiratory diseases in Iran: artificial neural network versus conditional logistic regression. *Int. J. Environ. Sci. Technol.* 2015;12:3433-3442.
8. Yu QL, Brouwers HJH. Indoor air purification using heterogeneous photocatalytic oxidation. Part I: Experimental study. *Appl. Catal. B-Environ.* 2009;192:454-461.
9. Yu K, Lee GWM, Huang W, Wu C, Yang S. The correlation between photocatalytic oxidation performance and chemical/physical properties of indoor volatile organic compounds. *Atmos. Environ.* 2006;40:375-385.
10. Bhatkhande DS, Pangarkar VG, Beenackers AACM. Photocatalytic degradation for environmental applications—A review. *J. Chem. Technol. Biotechnol.* 2001;77:102-116.
11. Subramonian W, Wu TY. Effect of enhancers and inhibitors on photocatalytic sunlight treatment of methylene blue. *Water Air Soil Poll.* 2014;225:1-15.
12. Low FCF, Wu TY, Teh CY, Juan JC. Investigation into photocatalytic decolorisation of CI Reactive Black 5 using titanium dioxide nanopowder. *Color Technol.* 2012;128:44-50.
13. Maggos T, Bartzis JG, Leva P, Kotzias D. Application of photocatalytic technology for NO_x removal. *Appl. Phys.* 2007;89:81-84.
14. Wu Z, Wang H, Liu Yue, Gu Z. Photocatalytic oxidation of nitric oxide with immobilized titanium dioxide films synthesized by hydrothermal method. *J. Hazard. Mater.* 2008;151:17-25.
15. Teh CY, Wu TY, Juan JC. Facile sonochemical synthesis of N,Cl-codoped TiO_2: Synthesis effects, mechanism and photocatalytic performance. *Catal. Today* 2015;256:365-374.
16. Dalton JS, Janes PA, Nicholson JA, Hallam KR, Allen GC. Photocatalytic oxidation of NO_x gases using TiO_2: a surface spectroscopic approach. *Environ. Pollut.* 2002;120:415-422.
17. Wang H, Wu Z, Zhao W, Guan B. Photocatalytic oxidation of nitrogen oxides using TiO_2 loading on woven glass fabric. *Chemosphere* 2007;66:185-190.
18. Ohama Y, Van Gemert D. Application of titanium dioxide photocatalysis to construction materials. London: Springer; 2011. p. 15-33.
19. Fujishima A, Rao TN, Tryk DA. Titanium dioxide photocatalysis. *J. Photochem. Photobiol. C: Photochem. Rev.* 2000;1:1-21.
20. Hashimoto K, Irie H, Fujishima A. TiO_2 photocatalysis: A historical overview and future prospects. *Jpn. J. Appl. Phys.* 2005;44:8269-8285.
21. Wang R, Hashimoto K, Fujishima A, et al. Watanabe, light-induced amphiphilic surfaces. *Nature* 1997;388:431-432.
22. Takeuchi M, Sakamoto K, Martra G, Coluccia S, Anpo M. Mechanism of photoinduced superhydrophilicity on the TiO_2 photocatalyst surface. *J. Phys. Chem. B* 2005;109:15422-15428.
23. Nakata K, Fujishima A. TiO_2 photocatalysis: Design and applications. *J. Photoch. Photobio. C: Photochem. Rev.* 2012;13:169-189.
24. Lasek J, Yu YH, Wu JCS. Removal of NO_x by photocatalytic processes. *J. Photochem. Rev.* 2013;14:29-52.
25. Asadi S, Hassan MM, Kevern JT, Rupnow TD. Development of pervious concrete pavement for air and storm water improvements. *Transp. Res. Rec.* 2015;2290:161-167.
26. Hassan MM, Dylla H, Asadi S, Mohammad LN, Cooper S. Laboratory evaluation of environmental performance of photocatalytic titanium dioxide warm-mix asphalt pavements. *J. Mater. Civ. Eng.* 2012;24:599-605.
27. Dylla H, Hassan MM, Mohammad L, Rupnow T. Evaluation of the environmental effectiveness of titanium dioxide photocatalyst coating for concrete pavements. *Transp. Res. Rec.* 2010;2164:46-51.
28. Sager M, Chon HT, Marton L. Spatial variation of contaminant elements of roadside dust samples from Budapest (Hungary) and Seoul (Republic of Korea), including Pt, Pd, and Ir. *Environ. Geochem. Health* 2015;37:191-193.
29. Davis AP. Field performance of bioretention: Water quality. *Environ. Eng. Sci.* 2007;24:1048-1064.
30. Vogel JR, Moore TL, Coffman RR, et al. Critical review of technical questions facing low impact development and green infrastructure: A perspective from the Great Plains. *Water Environ. Res.* 2015;87:849-862.
31. Yu YH, Pan YT, Wu J, Lasek J, Wu JCS. Photocatalytic NO reduction with C_3H_8 using a monolith photoreactor. *Catal. Today* 2011;174:141-147.
32. Ballari MM, Hunger M, Husken G, Brouwers HJH. NO_x photocatalytic degradation employing concrete pavement containing titanium dioxide. *Appl. Catal. B-Environ.* 2010;95:245-254.
33. ISO 22197-1: 2007, 'Fine ceramics, advanced technical ceramics) - Test method for air-purification performance of semiconducting photocatalytic materials - part 1: Removal of nitric oxide', ISO, Geneva; 2007.
34. Teleki A, Wengeler R, Wengeler L, Nirschl H, Pratsinis SE. Distinguishing between aggregates and agglomerates of flame-made TiO_2 by high-pressure dispersion. *Powder Technol.* 2008;181:292-300.
35. Nguyen NH, Bai H. Photocatalytic removal of NO and NO_2 using titania nanotubes synthesized by hydrothermal method. *J. Environ. Sci.* 2014;26:1180-1187
36. Ma J, Wu H, Liu Y, He H. Photocatalytic removal of NO_x over visible light responsive oxygen-deficient TiO_2. *J. Phys. Chem. C* 2014;118:7434-7441
37. Bowering N, Croston D, Harrison PG, Walker GS. Silver modified Degussa P25 for the photocatalytic removal of nitric oxide.

Int. J. Photoenergy 2007:1-8.
38. Guo G, Hu Y, Jiang S, Wei C. Photocatalytic oxidation of NO_x over TiO_2/HZSM-5 catalysts in the presence of water vapor: Effect of hydrophobicity of zeolites. *J. Hazard. Mater.* 2012;223-224:39-45.
39. Ichiura H, Kitaoka T, Tanaka H. Preparation of composite TiO_2-zeolite sheets using a papermaking technique and their application to environmental improvement. Part II: Effect of zeolite coexisting in the composite sheet on NO_x removal. *J. Mater. Sci.* 2003;38:1611-1615.